Annals of Botany **118**: 541–553, 2016
doi:10.1093/aob/mcw127, available online at www.aob.oxfordjournals.org

ANNALS OF BOTANY
Founded 1887

Optimal balance of water use efficiency and leaf construction cost with a link to the drought threshold of the desert steppe ecotone in northern China

Haixia Wei[1,*], Tianxiang Luo[1] and Bo Wu[2,*]

[1]*Key Laboratory of Alpine Ecology and Biodiversity, Institute of Tibetan Plateau Research, Chinese Academy of Sciences, Beijing 100101, China and* [2]*Institute of Desertification Studies, Chinese Academy of Forestry, Beijing 100091, China*
**For correspondence. Email weihaixia@itpcas.ac.cn or wubo@caf.ac.cn*

Received: 5 January 2016 Returned for revision: 17 March 2016 Accepted: 12 May 2016 Published electronically: 21 July 2016

• **Background and Aims** In arid environments, a high nitrogen content per leaf area (N_{area}) induced by drought can enhance water use efficiency (WUE) of photosynthesis, but may also lead to high leaf construction cost (CC). Our aim was to investigate how maximizing N_{area} could balance WUE and CC in an arid-adapted, widespread species along a rainfall gradient, and how such a process may be related to the drought threshold of the desert–steppe ecotone in northern China.
• **Methods** Along rainfall gradients with a moisture index (MI) of 0·17–0·41 in northern China and the northern Tibetan Plateau, we measured leaf traits and stand variables including specific leaf area (SLA), nitrogen content relative to leaf mass and area (N_{mass}, N_{area}) and construction cost (CC_{mass}, CC_{area}), $\delta^{13}C$ (indicator of WUE), leaf area index (LAI) and foliage N-pool across populations of *Artemisia ordosica*.
• **Key Results** In samples from northern China, a continuous increase of N_{area} with decreasing MI was achieved by a higher N_{mass} and constant SLA (reduced LAI and constant N-pool) in high-rainfall areas ($MI > 0{\cdot}29$), but by a lower SLA and N_{mass} (reduced LAI and N-pool) in low-rainfall areas ($MI \leq 0{\cdot}29$). While $\delta^{13}C$, CC_{mass} and CC_{area} continuously increased with decreasing MI, the low-rainfall group had higher N_{area} and $\delta^{13}C$ at a given CC_{area}, compared with the high-rainfall group. Similar patterns were also found in additional data for the same species in the northern Tibetan Plateau. The observed drought threshold where $MI = 0{\cdot}29$ corresponded well to the zonal boundary between typical and desert steppes in northern China.
• **Conclusions** Our data indicated that below a climatic drought threshold, drought-resistant plants tend to maximize their intrinsic WUE through increased N_{area} at a given CC_{area}, which suggests a linkage between leaf functional traits and arid vegetation zonation.

Key words: Carbon isotope, drought threshold, leaf area index, leaf trait relation, moisture index, sandy land, vegetation zonation, *Artemisia ordosica*.

INTRODUCTION

As aridity increases, drought-resistant plants (hereafter arid plants) tend to have a higher nitrogen content per leaf area (N_{area}, a ratio of mass-based nitrogen to specific leaf area, N_{mass}/SLA) (Cunningham *et al*., 1999; Wright *et al*., 2005; Cornwell *et al*., 2007), which can increase the water-use efficiency (WUE) of photosynthesis (Smith *et al*., 1997; Wright *et al*., 2001, 2003). While the positive relationship between N_{mass} and SLA generally exists across species and sites (Reich *et al*., 1997; Wright *et al*., 2004), higher N_{area} (i.e. higher N_{mass} at a given SLA, and vice versa) in species from low-rainfall areas could be achieved by higher N_{mass} or lower SLA, or both (Wright *et al*., 2001, 2003). Such a strategy shift in the SLA–N_{mass} relationship exists within the widespread species *Artemisia ordosica* along a rainfall gradient in northern China (Wei *et al*., 2011). Along a gradient of water availability, variations in leaf traits may arise from changes in leaf-level anatomical structure (Smith *et al*., 1997) and/or canopy foliage turnover and nitrogen allocation (Field, 1983; Farquhar *et al*., 2002) to maximize water- and nitrogen-use efficiencies. At the leaf level, the ultimate evolution of leaf form for arid plants tends towards a more cylindrical leaf with low SLA (i.e. high leaf thickness), which maximizes WUE by increasing the overlap area of light and CO_2 inside the leaf with few changes in the mesophyll conductance (Smith *et al*., 1997). Increased leaf thickness and decreased SLA associated with decreasing rainfall have been observed in previous studies (Witkowski and Lamont, 1991; Cunningham *et al*., 1999). At the stand level, the theoretical model for the simultaneous optimization of water- and nitrogen-use efficiencies of photosynthesis suggests that at a given total amount of canopy foliage N-pool, leaf area index (LAI) generally decreases as water becomes less available, resulting in a concomitant increase in N_{area} (N_{area} = N-pool/LAI) (Farquhar *et al*., 2002). Thus, in response to decreased rainfall, higher N_{area} within a widespread species may result from reduced LAI with unchanged foliage N-pool and SLA (Field, 1983; Farquhar *et al*., 2002; Wei *et al*., 2011), or from increased leaf thickness (i.e. lower SLA, Smith *et al*., 1997; Poorter *et al*., 2009) when the reduction of LAI can no longer compensate for soil water deficiency at low-rainfall sites. This suggests that maximizing N_{area} may be a key process

in shaping arid species' distribution and ecosystem function, and, if so, a drought threshold would exist associated with the switch change from allocating canopy leaf nitrogen to altering leaf-level anatomical structure along a rainfall gradient. However, little research has combined both theories to understand the intraspecific continuous variations in leaf traits and stand variables with rainfall. It is still unclear whether a drought threshold exists that causes a shift in controls on N_{area} across populations of an arid-adapted, widespread species along a large rainfall gradient. Such knowledge would help to understand the response of arid plants to climate change and to explore a simple predictor of arid vegetation zonation.

Leaf construction cost (CC) is defined as the amount of glucose required for constructing a unit leaf mass or leaf area (Williams *et al*., 1987). A leaf with low SLA or high N_{mass} generally has a high content of lignin or protein to resist environmental stress (Gower *et al*., 1989; Groeneveld *et al*., 1998; Zhang *et al*., 2012). These compounds (lignin and protein) are expensive to produce (Williams *et al*., 1987; Nagel and Griffin, 2001). To maximize N_{area} for high WUE, the induction of a low SLA and/or high N_{mass} by drought may also increase CC (Penning de Vries *et al*., 1974; Williams *et al*., 1987; Griffin, 1994; Nagel and Griffin, 2001; Nagel *et al*., 2002; Chen *et al*., 2006; Zhang *et al*., 2012). Higher CC is usually associated with lower energy-use efficiency and growth rate (Griffin, 1994; Poorter and Villar, 1997; Baruch and Goldstein, 1999; Nagel *et al*., 2004; Song *et al*., 2007), which may hinder plant survival and competition with other species in arid environments. It has been suggested that arid plants have to balance the costs of carbon gain and water transport along a rainfall gradient by altering their leaf traits (Wright *et al*., 2003; Prentice *et al*., 2014). The regulation of N_{area} along a rainfall gradient should be a process to balance WUE and CC, although it is still unknown how maximizing N_{area} could achieve this in arid-adapted species.

In arid and semi-arid sandy lands in northern China (1200–1800 m) and in the south-east Qaidam Basin of Qinghai (3200–3300 m), the deciduous sub-shrub *A. ordosica* is widely distributed in mild and moderately disturbed (fixed and semi-fixed, respectively) sandy lands across a broad range of annual rainfall (150–400 mm). The Mu Us Sandy Land is the distribution centre of *A. ordosica*, where mean air temperature and soil texture are similar across areas with differing rainfall (Wei *et al*., 2011). Moreover, there is no significant genetic differentiation among *A. ordosica* populations from divergent geographical zones (Wang *et al*., 2004). Such a species distribution pattern provides an ideal system for identifying the drought threshold and related mechanisms of the intraspecific shift in controls on N_{area} along a rainfall gradient. In this study, leaf traits (SLA, N_{mass}, N_{area}, CC_{mass}, CC_{area}, $\delta^{13}C$) and related stand variables (LAI and foliage N-pool) within populations of *A. ordosica* were measured across 17 study sites in the Mu Us Sandy Land and its neighbouring areas with annual rainfall ranging from 150 to 370 mm. Our aim was to test the hypothesis that below a climatic drought threshold, arid plants tend to maximize their intrinsic WUE (i.e. high leaf $\delta^{13}C$, Farquhar *et al*., 1989) through increased N_{area} at a given CC_{area}. We investigated: (1) whether there is a drought threshold determining the significant shift in SLA–N_{mass} relationships and, if so, whether this drought threshold also determines the turning point in leaf traits and stand variables along the rainfall gradient; (2) if the positive relationship between N_{area} and CC_{area} also shifts between low- and high-rainfall groups consistent with the pattern found in the SLA–N_{mass} relationship, and whether the low-rainfall group has higher N_{area} and $\delta^{13}C$ at a given CC_{area} compared with the high-rainfall group; and (3) if the drought threshold identified by leaf-trait data could indicate the zonal boundary between typical temperate and desert steppes in northern China. Furthermore, we investigated the generality of the low-altitude data from northern China using the high-altitude data from the south-east Qaidam Basin of Qinghai.

MATERIALS AND METHODS

Study sites

Artemisia ordosica is adapted to fixed and semi-fixed sandy land habitats across typical temperate steppes, desert steppes and semi-deserts in northern China, where annual rainfall ranges from 150 to 400 mm (Fig. 1) (Cui, 1991; Wang *et al*., 2002). *Artemisia ordosica* is a dominant species that forms a relatively stable community in sub-climax state in the mild and moderately degraded Mu Us Sandy Land and its neighboring areas that are characterized by arid and infertile soils. Soil textures at 0–50 cm depth are similar across different rainfall areas, with sand contents of > 96 % and clay contents of < 4 % across fixed and semi-fixed sandy lands (Duan and Liu, 1995; Chen *et al*., 1998; Wang, 2006; Li, 2007). We selected our study sites by overlapping the geographical distribution of *A. ordosica* with the map of annual rainfall isolines in northern China. Along a geographical transect from east to west in the Mu Us Sandy Land and its neighbouring areas, we selected 17 study sites (four of which are presented in Wei *et al*., 2011) to represent 17 different rainfall areas (Fig. 1). Locations and altitudes of the 17 study sites were recorded by a global positioning system, with latitudes of 37°27′40″–39°43′57″N, longitudes of 102°46′33″–109°52′06″E and altitudes of 1210–1783 m (Table 1).

Daily meteorological data (1985–2010) for 142 meteorological stations in northern China were obtained from China's National Meteorological Bureau. The meteorological data included atmospheric pressure (Pa), vapour pressure (Pa), mean air temperature (°C), maximum air temperature (°C), minimum air temperature (°C), mean relative humidity (%), sunshine duration (h), wind speed (m s^{-1}) and rainfall (mm). Annual potential evapotranspirations for the 142 meteorological stations were calculated with the Penman–Montieth equation (Allen *et al*., 1998). Moisture index (MI) was then calculated as the ratio of annual rainfall to annual potential evapotranspiration. The isoline maps of annual mean temperature, rainfall, potential evapotranspiration and MI were produced with the Krige spatial interpolation method. The climate data (averaged over 1985–2010) of the 17 study sites were estimated according to the geographical locations. Across the 17 study sites, annual mean temperature was 7·5–9·4 °C, annual rainfall 150–370 mm, annual potential evapotranspiration 867–965 mm and MI 0·17–0·41 (Table 1).

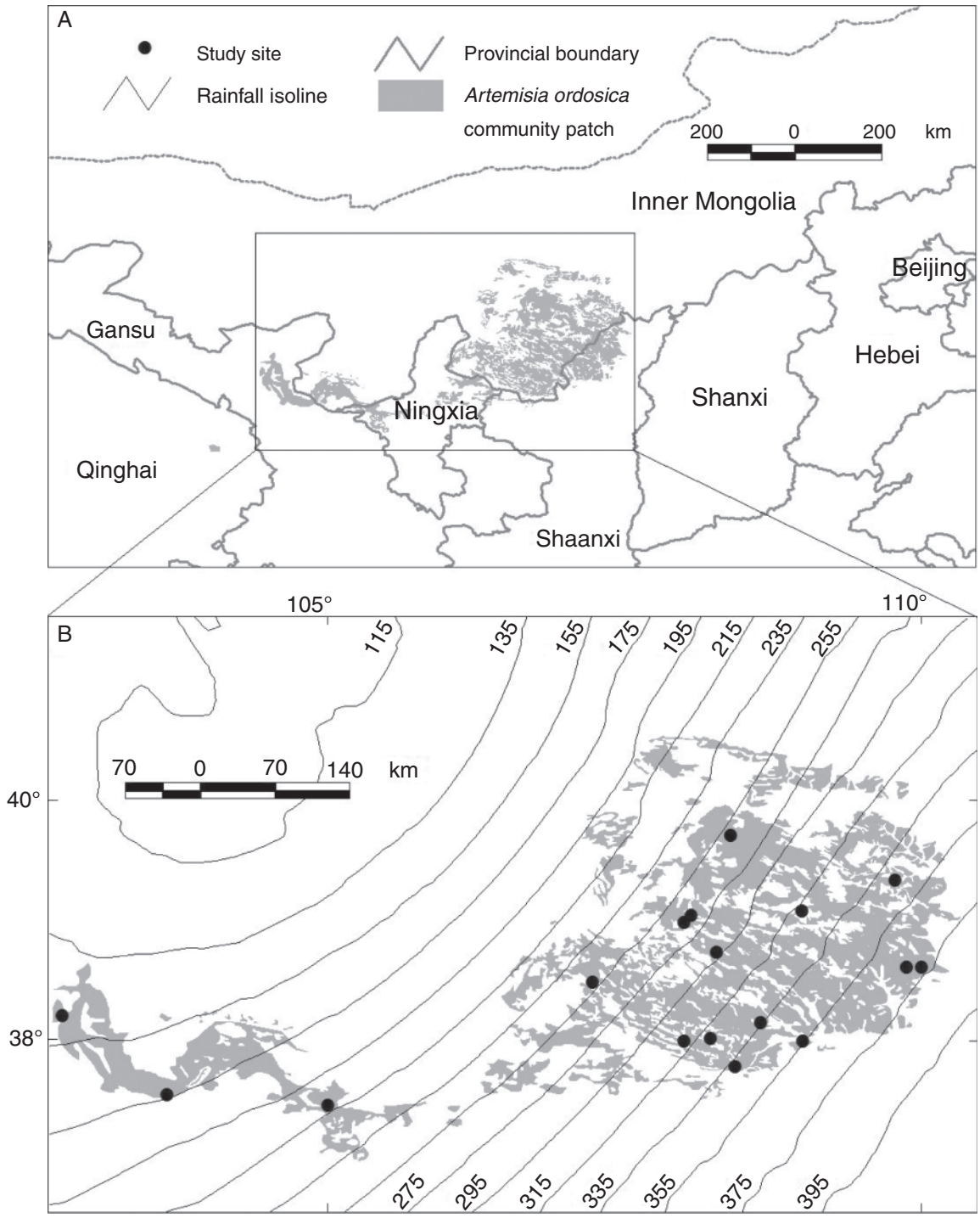

FIG. 1. Location of study areas (A) and map of the geographical distribution of *A. ordosica* and annual rainfall isolines (B). The geographical distribution of *A. ordosica* was adapted from the Vegetation Map of China (Zhang, 2007).

Sampling and measurement of leaf traits

At each study site, leaf and soil samples were collected at both fixed and semi-fixed sandy land habitats, which were identified according to differences in vegetation cover (> 40 vs. 20–40 %, respectively) and soil crust thickness (>1 vs. 0·5–1 cm, respectively) (Wu and Ci, 2002). During July and August when leaves were fully expanded, the outer-canopy leaves of nine healthy *A. ordosica* individuals were sampled from three 5 × 5-m plots per habitat.

For each plant individual sampled, 50 fresh leaves were scanned with a conventional digital scanner (HP Scanjet 2400, Hewlett Packard Company, Palo Alto, CA, USA) and

calibrated with a square of known surface area. We determined single-sided leaf area from scanned images using Image Pro Plus 6.0 software (Media Cybemetics Inc., New York, USA). SLA was calculated as the fresh leaf area divided by its dry mass (oven-dried for 48 h at 70 °C). Leaf N_{mass} was analysed using the Kjeldahl method (Kjeldahl, 1883) and N_{area} was calculated as the ratio of N_{mass} to SLA. The $\delta^{13}C$ ratio of leaf samples, relative to a Pee Dee Belemnite (PDB) standard, was

TABLE 1. *Climate and soil factors of study sites across northern China and the south-east Qaidam Basin sandy lands*

Site number	Place name	Longitude	Latitude	Altitude (m)	MAP (mm)	MAE (mm)	MI	MAT (°C)	Total soil N concentration (mg g^{-1})	
									Fixed sandy land	Semi-fixed sandy land
Northern China sandy lands										
1	Yulin	109°52′06″	38°37′18″	1213	367	902	0·41	8·4	$0·55\pm0·064^{aA}$	$0·17\pm0·043^{bAB}$
2	Ejin Horo	109°46′26″	39°21′17″	1350	342	881	0·39	7·5	$0·55\pm0·170^{aAB}$	$0·18\pm0·016^{bA}$
3	Uxin Henan	108°25′36″	37°47′27″	1307	336	946	0·36	9	$0·37\pm0·172^{aBC}$	$0·10\pm0·014^{bC}$
4	Uxin	108°38′36″	38°09′28″	1270	331	930	0·36	8·7	$0·40\pm0·013^{aB}$	$0·17\pm0·022^{bAB}$
5	Otog Qian	108°13′26″	38°1′17″	1380	320	947	0·34	8·7	$0·41\pm0·110^{aB}$	$0·09\pm0·053^{bC}$
6	Uxin Ju	108°59′40″	39°05′54″	1295	318	903	0·35	7·9	$0·51\pm0·087^{aAB}$	$0·08\pm0·014^{bC}$
7	Otog Sumitu	108°16′34″	38°44′53″	1361	290	929	0·31	8·1	$0·45\pm0·142^{aAB}$	$0·12\pm0·008^{bBC}$
8	Otog	108°03′30″	39°03′37″	1419	265	923	0·29	7·8	$0·35\pm0·099^{aBC}$	$0·21\pm0·017^{bA}$
9	Hangjin	108°23′45″	39°43′57″	1410	258	900	0·29	7·8	$0·36\pm0·029^{aBC}$	$0·18\pm0·014^{bA}$
10	Otogqian Damiao	107°13′49″	38°29′46″	1431	250	965	0·26	8·7	$0·32\pm0·036^{aCD}$	$0·21\pm0·086^{bA}$
11	Shapotou	105°00′28″	37°27′40″	1267	210	917	0·23	9·4	$0·17\pm0·051^{aE}$	$0·07\pm0·008^{bC}$
12	Gulang	103°39′22″	37°33′03″	1783	172	851	0·20	9·1	$0·20\pm0·050^{aE}$	$0·10\pm0·036^{bC}$
13	Minqin	102°46′33″	38°12′57″	1444	150	867	0·17	8·8	$0·13\pm0·033^{aE}$	$0·06\pm0·008^{bC}$
14*	Yulin	109°51′57″	38°37′26″	1210	370	898	0·41	8·6	$0·28\pm0·049^{aD}$	$0·18\pm0·075^{bAB}$
15*	Uxin	108°38′30″	38°09′38″	1270	353	931	0·38	8·7	$0·24\pm0·012^{aDE}$	$0·07\pm0·016^{bC}$
16*	Otogqian Chengchuan	108°27′22″	37°42′17″	1320	310	950	0·33	8·8	$0·32\pm0·052^{aCD}$	$0·19\pm0·038^{bA}$
17*	Otog	108°03′30″	39°03′38″	1420	264	923	0·29	7·6	$0·37\pm0·039^{aBC}$	$0·19\pm0·018^{bA}$
South-east Qaidam Basin sandy lands										
18*	Qinghai Lake	100°46′48″	36°43′53″	3289	401	592	0·68	0·4	$0·22\pm0·049^{aDE}$	$0·14\pm0·034^{aB}$
19*	Dulan	98°11′51″	36°15′54″	3284	207	835	0·25	3·5	$0·18\pm0·059^{aE}$	$0·11\pm0·012^{aBC}$

Different letters within a row and a column show significant differences between each site's sandy land habitats (lowercase) and between study sites (uppercase) at a 0·05 level, respectively. MAP, mean annual precipitation; MAE, mean annual potential evapotranspiration; MAT, mean annual temperature; MI = MAP/MAE, moisture index.

*Data from Wei *et al*. (2011).

TABLE 2. *Differences in slopes and intercepts of* N_{mass}*–SLA relationships for* A. ordosica *among 17 study sites and three rainfall groups in northern China sandy lands*

Site/group	MI	Slope			Intercept		
		Total	FS	SFS	Total	FS	SFS
Northern China sandy lands							
1	0·41	$0·17^{a}$	$0·18^{a}$	$0·16^{a}$	$6·4^{c}$	$5·7^{c}$	$6·4^{c}$
2	0·39	$0·22^{a}$	$0·20^{a}$	—	$-0·01^{c}$	$4·0^{c}$	—
3	0·36	$0·12^{a}$	—	$0·18^{a}$	$8·7^{c}$	—	$4·4^{c}$
4	0·36	$0·11^{a}$	—	$0·24^{a}$	$11·7^{c}$	—	$0·42^{c}$
5	0·34	$0·21^{a}$	$0·15^{a}$	$0·26^{a}$	$2·0^{c}$	$9·6^{c}$	$-4·3^{c}$
6	0·35	$0·21^{a}$	$0·20^{a}$	$0·21^{a}$	$2·4^{c}$	$4·3^{c}$	$1·8^{c}$
7	0·31	$0·19^{a}$	$0·28^{a}$	$0·14^{a}$	$9·1^{b}$	$0·99^{b}$	$13·5^{b}$
8	0·29	$0·17^{a}$	$0·15^{a}$	$0·16^{a}$	$15·6^{a}$	$16·7^{a}$	$17·9^{a}$
9	0·29	$0·09^{a}$	$0·09^{a}$	$0·08^{a}$	$24·9^{a}$	$24·8^{a}$	$25·7^{a}$
10	0·26	$0·25^{a}$	—	$0·20^{a}$	$9·5^{a}$	—	$15·4^{a}$
11	0·23	$0·15^{a}$	$0·17^{a}$	$0·15^{a}$	$14·8^{a}$	$13·4^{a}$	$15·3^{a}$
12	0·20	$0·19^{a}$	$0·14^{a}$	—	$12·5^{a}$	$17·4^{a}$	—
13	0·17	$0·24^{a}$	—	$0·16^{a}$	$9·6^{a}$	—	$18·5^{a}$
14	0·41	$0·16^{a}$	$0·28^{a}$	—	$6·1^{c}$	$-2·9^{c}$	—
15	0·38	$0·21^{a}$	—	$0·23^{a}$	$3·1^{c}$	—	$1·5^{c}$
16	0·33	$0·10^{a}$	—	—	$12·8^{c}$	—	—
17	0·29	$0·18^{a}$	—	—	$16·2^{a}$	—	—
Group 1 (sites 1–6, 14–16)	0·33–0·41	$0·17^{a}$	$0·19^{a}$	$0·22^{a}$	$6·0^{c}$	$5·0^{c}$	$1·6^{c}$
Group 2 (site 7)	0·31	$0·19^{a}$	$0·28^{a}$	$0·14^{a}$	$9·1^{b}$	$0·99^{b}$	$13·5^{b}$
Group 3 (sites 8–13, 17)	0·17–0·29	$0·22^{a}$	$0·18^{a}$	$0·18^{a}$	$11·7^{a}$	$14·5^{a}$	$14·9^{a}$

Data analysis was performed by ANCOVA. Different letters within a column show significant differences between study sites or between rainfall groups at a 0·05 level. MI, moisture index; Total, in pooled data from FS and SFS; FS, fixed sandy land; SFS, semi-fixed sandy land.

determined by combusting samples in an elemental analyser coupled to a stable isotope mass spectrometer (Flash EA + Delta V, Thermo Fisher Scientific Inc., Waltham, MA, USA). The overall precision of the $\delta^{13}C$ analysis was 0·1.

For each leaf sample, the heat of combustion (HC) was measured with an oxygen bomb calorimeter (PARR 1281, Parr Instrument Company, Moline, IL, USA). The HC for each sample was determined in triplicate, with the relative differences among the three measurements being <2 %. The ash concentration (AC) was determined by combustion of 1-g leaf samples in a muffle furnace at 550 °C for 4 h until a white–grey residue remained. Mass-based leaf construction cost (CC_{mass}) was calculated by the formula given by Williams *et al.* (1987):

$$CC_{mass} = [(0 \cdot 06968HC - 0 \cdot 065)\ (1 - AC) + 7 \cdot 5062(kN/14 \cdot 0067)]/E_G$$

where CC_{mass} = construction cost (g glucose g^{-1}), HC = heat of combustion (kJ g^{-1}), AC = total ash content (%), k is the oxidation state of the N source (+5 for nitrate or –3 for ammonium), N = total Kjeldah nitrogen (g g^{-1}), and E_G is a constant of 0·89 (Williams *et al.*, 1987). In this study, we calculated CC_{mass} with $k = 5$, as nitrate is the principal source of nitrogen that is available to terrestrial plants under most field conditions (Taiz and Zeiger, 1991). CC_{area} was calculated as the ratio of CC_{mass} to SLA.

Measurement of stand and soil variables

Within each of the 102 plots across the 17 study sites, we measured the crown diameters along the maximum and minimum axes for each *A. ordosica* individual clump and then calculated the projected area of a crown as the elliptical area. At each study site, 18 individual clumps of *A. ordosica* with different crown areas were harvested for measurements of foliage dry mass per clump. Allometric regression equations were developed between foliage mass and crown area for each study site. The foliage biomass of *A. ordosica* within each plot was then estimated according to the allometric equations using the clump-specific crown area measurements. LAI and foliage N-pool were calculated as the foliage biomass multiplied by SLA and N_{mass}, respectively.

For each plot, two soil samples (0–10 and 20 cm in depth) were collected and analysed for soil total nitrogen concentration (STN) using the Kjeldahl method (Kjeldahl, 1883).

Additional data from the south-east Qaidam Basin

Wei *et al.* (2011) indicated that the drought-induced shift in the SLA–N_{mass} relationship was also found in the data from the south-east Qaidam Basin of Qinghai. To test the generality of the CC and $\delta^{13}C$ data found in the low-altitude regions of northern China, we also measured these two traits in *A. ordosica* individuals across two high-altitude sandy lands in Dulan and Qinghai Lake within the south-east Qaidam Basin, using the leaf samples collected by Wei *et al.* (2011). The methods of leaf sampling and measurements were the same as described above. According to climate data obtained from the

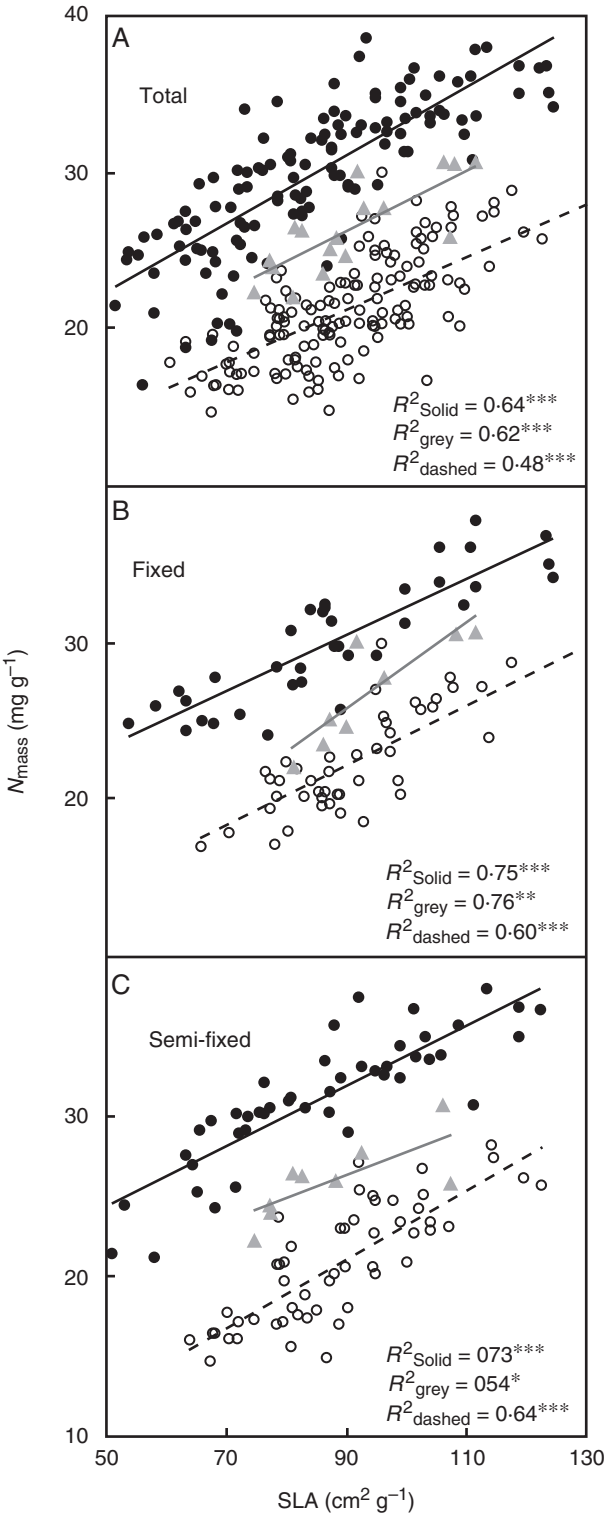

FIG. 2. Strategy shifts in SLA–N_{mass} relationships for *A. ordosica* along a rainfall gradient in northern China sandy lands. Data analyses were performed on pooled data (A) and for fixed (B) and semi-fixed (C) sandy land habitats, respectively. Empty circles and dashed trend lines are for high-rainfall areas (rainfall group 1, 310–370 mm; MI, 0·33–0·41); grey triangles and trend lines are for mid-rainfall transition (rainfall group 2, 290 mm; MI, 0·31); filled circles and solid trend lines are for low-rainfall areas (rainfall group 3, 150–265 mm; MI, 0·17–0·29). ANCOVA statistics are given in Table 2.

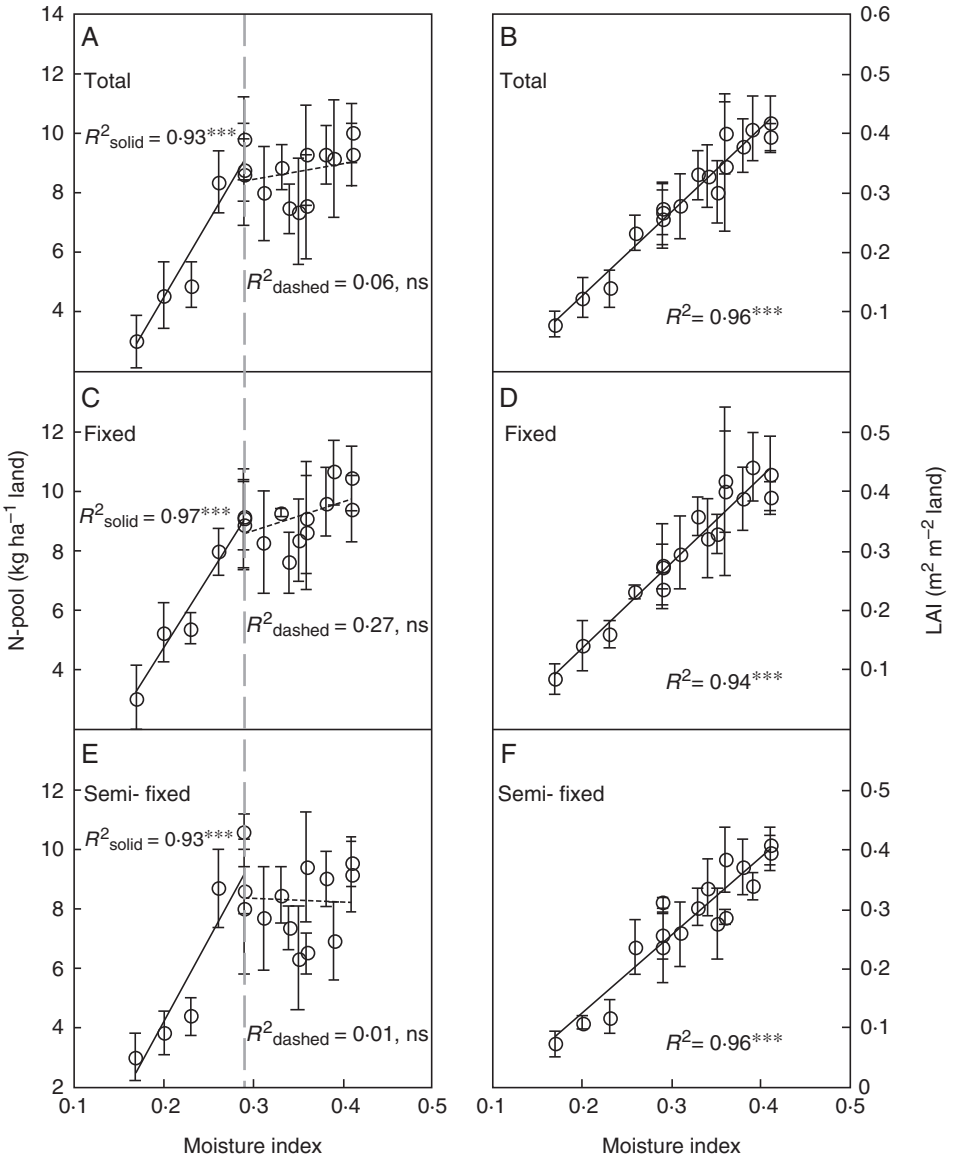

FIG. 3. Variations in stand-level foliage N-pool (A, C, E) and LAI (B, D, F) for *A. ordosica* populations along an MI gradient in northern China sandy lands. Data analyses were performed on pooled data (A, B) and for fixed (C, D) and semi-fixed (E, F) sandy land habitats, respectively. (A, C, E) Grey dashed lines indicate a climatic drought threshold with MI = 0·29, and the relationships between foliage N-pool and MI differ below and above the drought threshold; the solid trend lines are for the areas with MI ≤ 0·29 and the dashed trend lines are for the areas with MI > 0·29. Bars indicate mean ± s.d.

Dulan and Qinghai Lake stations, the calculated MI was 0·25 in Dulan and 0·68 in Qinghai Lake (Table 1).

Data analysis

One-way analysis of variance (ANOVA) was applied to assess differences in leaf traits and STN between the two sandy land habitats per site and between 17 study sites. If the results of the ANOVA were significant, Tukey's pair-wise comparisons were made.

A simple linear model ($y = a + bx$) was used for analysing bivariate relationships of leaf traits. Analysis of covariance (ANCOVA) in a general linear model framework was applied to test for differences in the slopes and intercepts of SLA–N_{mass} relationships from different rainfall areas, in which rainfall served as a grouping variable, N_{mass} as a dependent variable and SLA as a covariate. We tested first for the homogeneity of slopes and then for the difference in intercepts. Data from different rainfall areas were pooled as a rainfall group if there were not significant differences in slopes and intercepts. In this way, a drought threshold was determined by the significant shift in the SLA–N_{mass} relationship along the rainfall gradient. Accordingly, differences in slopes and intercepts for relationships of N_{area}-CC_{area} and $\delta^{13}C$-N_{area} among different rainfall groups (identified by the SLA–N_{mass} relationship) were further tested with ANCOVA in a general linear model framework. The relationships of leaf traits (SLA, N_{mass}) and stand variables (LAI, foliage N-pool) with MI below and above the drought threshold were also analysed by a simple linear model ($y = a + bx$).

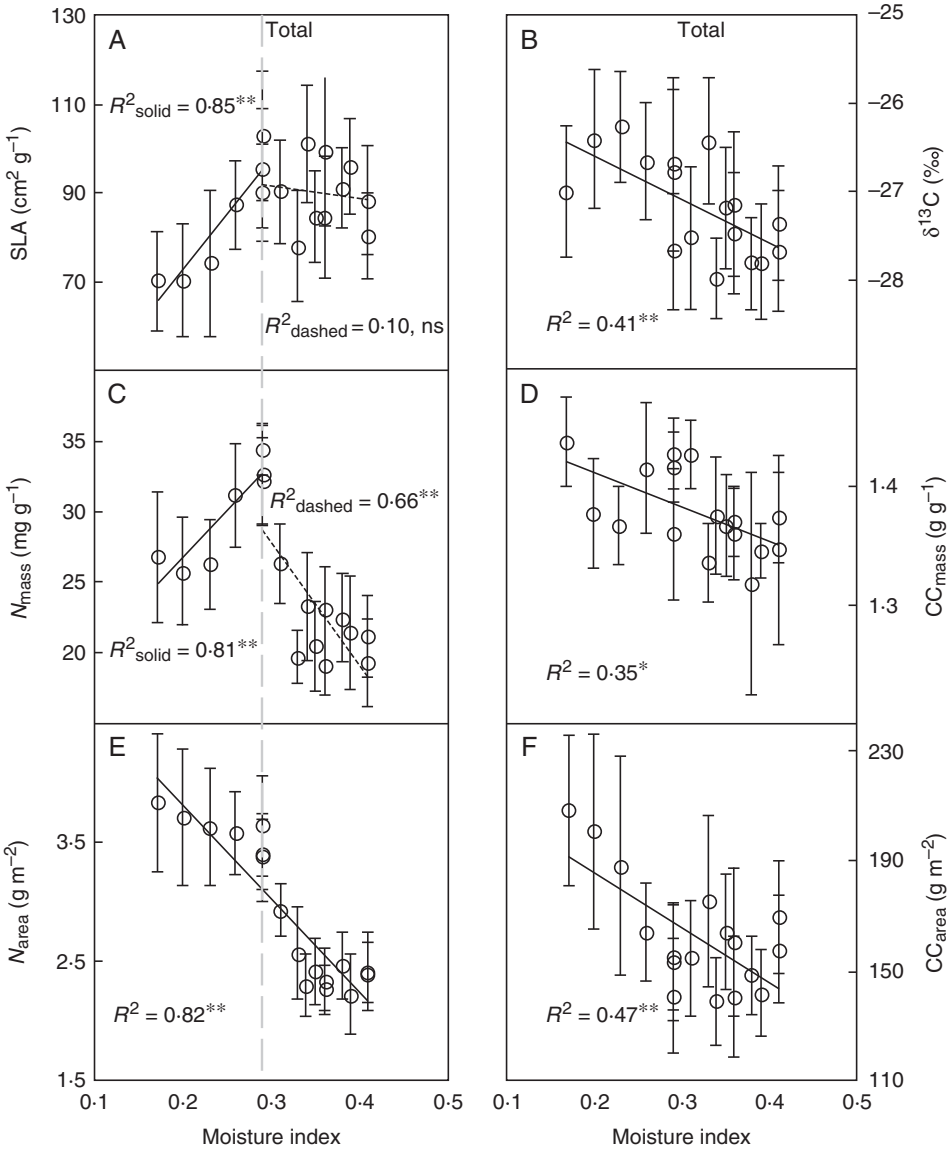

FIG. 4. Variations in SLA (A), N_{mass} (C), N_{area} (E), δ^{13}C (B), CC_{mass} (D) and CC_{area} (F) for *A. ordosica* along an MI gradient in northern China sandy lands. Data analyses were performed on pooled data from fixed and semi-fixed sandy land habitats. (A, C) Grey dashed lines indicate a climatic drought threshold with MI = 0·29, and the relationships of SLA (A) and N_{mass} (C) to MI differ below and above the drought threshold; the solid trend lines are for the areas with MI ≤ 0·29 and the dashed trend lines are for the areas with MI > 0·29. Bars indicate mean ± s.d.

At each of the 17 study sites in northern China, there were significant differences in STN between the two sandy land habitats. STN increased with increasing MI in fixed sandy lands ($P < 0·01$) but varied little in semi-fixed sandy lands ($P = 0·30$) (Table 1). To examine the effect of STN on the leaf-trait relationships, data analyses were performed for fixed and semi-fixed sandy land habitats and as well as in pooled data. The drought threshold identified by leaf trait data was then compared with the zonal boundary between typical temperate and desert steppes by overlapping the map of vegetation zonations in Zhang (2007) with the map of the MI isolines in northern China.

The statistical analysis was performed using SPSS 16.0 for Windows (SPSS Inc., Chicago, IL, USA), and all significant differences were taken at $P < 0·05$.

RESULTS

Drought threshold indicating a shift in the SLA–N_{mass} relationship and its link to stand variables along the rainfall gradient

Across the two sandy land habitats and in pooled data, there were no differences in individual SLA–N_{mass} slopes among the 17 study sites ($P = 0·40$–$0·66$) (Table 2). However, the SLA–N_{mass} intercepts showed significant differences between the three rainfall groups ($P < 0·001$): high-rainfall areas (rainfall group 1, 310–370 mm; MI = 0·33–0·41), mid-rainfall transition (rainfall group 2, 290 mm; MI = 0·31) and low-rainfall areas (rainfall group 3, 150–265 mm; MI = 0·17–0·29) (Fig. 2, Table 2). In general, the SLA–N_{mass} relationship shifted significantly

between low-rainfall areas and high-rainfall areas with a transition in between (Fig. 2).

Regardless of STN variability, the relationship between foliage N-pool and MI differed below and above the drought threshold. Canopy foliage N-pool increased with increasing MI in areas with MI $\leq$ 0·29 ($P < 0·001$) but varied little in areas with MI > 0·29 ($P = 0·07$–$0·89$) (Fig. 3A, C, E). However, LAI generally increased with increasing MI in a continuously linear model along the entire rainfall gradient ($P < 0·001$) (Fig. 3B, D, F). In pooled data, leaf-level SLA and N_{mass} increased with increasing MI in areas with MI $\leq$ 0·29 ($P < 0·01$). In areas with MI > 0·29, N_{mass} decreased with increasing MI ($P < 0·01$) while SLA varied little ($P = 0·29$) (Fig. 4A, C). As a result, N_{area} (N_{mass}/SLA or N-pool/LAI) decreased continuously with increasing MI along the entire rainfall gradient ($P < 0·001$) (Fig. 4E). Because N_{area} and $\delta^{13}C$ were positively correlated with CC and its major components of HC and N_{mass} (Table 3), $\delta^{13}C$, CC_{mass} and CC_{area} generally showed a continuously decreasing trend with increasing MI ($P < 0·05$) (Fig. 4B, D, F). The same patterns were also found in fixed and semi-fixed sandy land habitats (Supplementary Data, Figs S1 and S2, respectively).

Shifts in relationships of N_{area} to CC_{area} and $\delta^{13}C$ between low- and high-rainfall areas

Across the sandy land habitats and in the pooled data, the positive relationship of N_{area} to CC_{area} also shifted between low-rainfall areas and high-rainfall areas along the rainfall gradient in northern China (Fig. 5A, C, E and Table 4, test for slopes, $P = 0·12$–$0·45$; test for intercepts, $P < 0·001$). The plants in low-rainfall areas had higher N_{area} at a given CC_{area} compared with those in high-rainfall areas (Fig. 5A, C, E). Similar patterns were also found in the south-east Qaidam Basin (Fig. 6A, C, E and Table 4, test for slopes, $P = 0·71$; test for intercepts, $P < 0·05$).

There was a positive N_{area}–$\delta^{13}C$ relationship with insignificant differences of slopes and intercepts between low- and high-rainfall areas in northern China (Table 5, test for slopes, $P = 0·09$–$0·62$; test for intercepts, $P = 0·28$–$0·96$). In contrast to strategy shifts in relationships of SLA–N_{mass} and N_{area}–CC_{area} between low- and high-rainfall areas, there was a continuous positive relationship between N_{area} and $\delta^{13}C$ along the entire rainfall gradient ($P < 0·001$) (Fig. 5B, D, F). Similar patterns were also found in additional data from the south-east Qaidam Basin ($P < 0·05$) (Fig. 6B, D, F).

The drought threshold for the boundary between typical and desert steppes

The drought threshold where MI = 0·29 identified by leaf-trait data of *A. ordosica* corresponded well to the zonal boundary between typical and desert steppes in northern China (Fig. 7). The sites from the high-rainfall group were distributed in the typical steppe zone in the east, while the sites from the low-rainfall group were from the desert steppe and semi-desert zones in the west (Fig. 7).

TABLE 3. *Pearson correlation coefficients between leaf traits (SLA, N_{area} and $\delta^{13}C$) and CC and its components (HC, AC and N_{mass}) in leaf samples of* A. ordosica *collected from 17 study sites in northern China sandy lands*

CC and its components	SLA	N_{area}	$\delta^{13}C$
Total ($n = 281$)			
HC	−0·17**	0·22***	0·25***
AC	−0·02	−0·12*	−0·15*
N_{mass}	0·37***	0·65***	0·34***
CC_{mass}	0·02	0·41***	0·35***
CC_{area}	−0·94***	0·53***	0·23***
Fixed sandy land ($n = 144$)			
HC	−0·24**	0·12	0·10
AC	−0·02	0·01	0·05
N_{mass}	0·32***	0·60***	0·32***
CC_{mass}	−0·08	0·28**	0·17*
CC_{area}	−0·94***	0·61***	0·20*
Semi-fixed sandy land ($n = 137$)			
HC	−0·09	0·31***	0·36***
AC	−0·03	−0·25**	−0·32***
N_{mass}	0·41***	0·70***	0·36***
CC_{mass}	0·10	0·53***	0·47***
CC_{area}	−0·95***	0·45***	0·28**

*$P < 0·05$,
**$P < 0·01$,
***$P < 0·001$.

DISCUSSION

Maximizing N_{area} is a process to balance WUE and CC in arid plants along a rainfall gradient

To the best of our knowledge, few studies have examined the intraspecific continuous variations in leaf traits and related stand variables along a rainfall gradient. Our data demonstrated that a continuous increase in N_{area} with decreasing rainfall was achieved by a reduced LAI with unchanged foliage N-pool and SLA (higher N_{mass} and constant SLA) in high-rainfall areas with MI > 0·29, but by an increased leaf thickness (lower SLA and N_{mass}) in low-rainfall areas with MI $\leq$ 0·29 (Figs 2–4). The results indicate a drought threshold where MI = 0·29 determines the shift in controls on N_{area} associated with the switch change from allocating canopy leaf nitrogen to altering leaf-level anatomical structure along a rainfall gradient, which can be explained by the theories of Farquhar *et al.* (2002) and Smith *et al.* (1997). Such a drought threshold is close to the reported aridity threshold in controlling ecosystem nitrogen cycling of temperate grasslands in northern China (MI = 0·32, Wang *et al.*, 2014).

Our transect data further indicated that relationships of N_{area}–CC_{area} consistently shifted between low-rainfall areas and high-rainfall areas (Fig. 5), which was confirmed by additional data from the south-east Qaidam Basin (Fig. 6). Because there was a continuous positive relationship between N_{area} and $\delta^{13}C$ and both generally increased with decreasing MI along the entire rainfall gradient, the low-rainfall group had higher N_{area} and $\delta^{13}C$ at a given CC_{area} compared with the high-rainfall group. Our data supported the hypothesis that below a climatic drought threshold, arid plants tend to maximize their intrinsic WUE

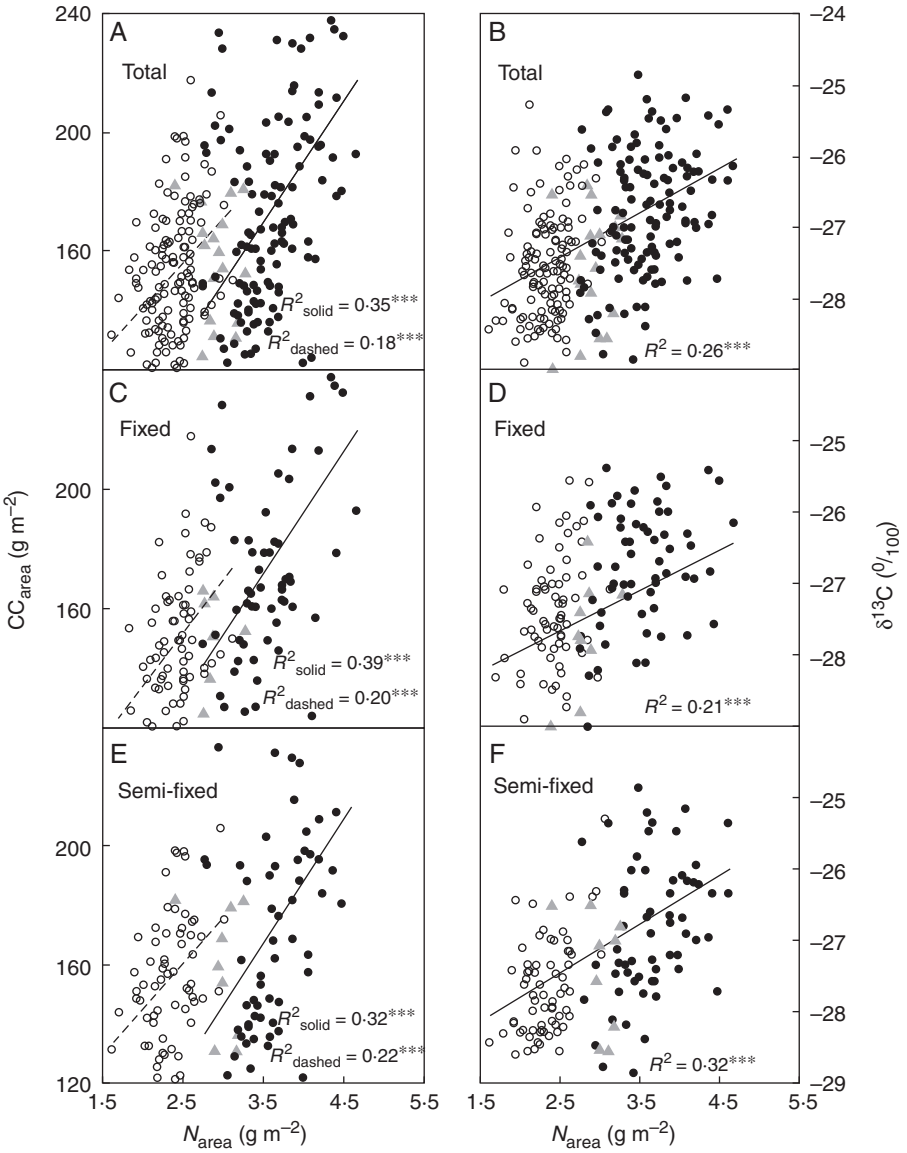

FIG. 5. Relationships of N_{area} to CC_{area} (A, C, E) and $\delta^{13}C$ (B, D, F) for *A. ordosica* along a rainfall gradient in northern China sandy lands. The N_{area}–CC_{area} relationships (A, C, E) shift between high-rainfall areas (rainfall group 1, 310–370 mm; MI, 0·33–0·41) and low-rainfall areas (rainfall group 3, 150–265 mm; MI, 0·17–0·29), contrasting with the continuous relationships of N_{area}–$\delta^{13}C$ (B, D, F) along the entire rainfall gradient. Data analyses were performed on pooled data (A, B) and for fixed (C, D) and semi-fixed (E, F) sandy land habitats, respectively. Symbols are as in Fig. 2. ANCOVA statistics are given in Tables 4 and 5.

($\delta^{13}C$) through increased N_{area} at a given CC_{area}. Such ecophysiological mechanisms may explain why *A. ordosica* can be widely distributed in arid sandy lands and how it forms a relatively stable community in a sub-climax state. Our findings suggest that maximizing N_{area} for optimal balance of WUE and CC is a key process in shaping arid species distribution and ecosystem function.

Variations of CC along an environmental gradient may be determined by changes in leaf biochemical composition and leaf morphology (Griffin, 1994). There are still ongoing debates about how CC changes in response to environmental stress (Chapin, 1989; Poorter and De Jong, 1999; Villar and Merino, 2001; Martínez *et al*., 2002). Several studies have suggested that there is an increase in CC under stress conditions (Penning de Vries *et al*., 1974; Amthor, 1989), while Merino (1987) found that water availability has no effects on the CC of 30 species in the Mediterranean. In this study, the $\delta^{13}C$, CC_{mass} and CC_{area} of *A. ordosica* continuously increased with decreasing MI along the rainfall gradient. This suggests that maximizing N_{area} for high WUE inevitably leads to a high CC, which is consistent with the theoretical model prediction of Prentice *et al*. (2014), suggesting that altering leaf-level anatomical structure might be more costly than allocating canopy leaf nitrogen.

To further investigate the possible effect of soil texture on the shifts in leaf trait relationships between low- and high-rainfall areas, the literature data on soil texture across 23 sandy land sites located in our study areas were obtained from Li (2007).

TABLE 4. *Differences in slopes and intercepts of CC_{area}–N_{area} relationships for* A. ordosica *between low- and high-rainfall groups across northern China and the south-east Qaidam Basin sandy lands*

Group/site	MI	Slope			Intercept		
		Total	FS	SFS	Total	FS	SFS
Northern China sandy lands							
Group 1, 0·33–0·41		33·7[a]	36·4[a]	35·6[a]	73·1[a]	61·9[a]	73·8[a]
Group 3, 0·17–0·29		47·6[a]	46·9[a]	49·9[a]	1·8[b]	7·4[b]	–9·7[b]
South-east Qaidam Basin sandy lands							
Qinghai Lake, 0·68		40·0[a]	–	47·8[a]	96·9[a]	–	87·3[a]
Dulan, 0·25		32·0[a]	–	38·3[a]	92·6[b]	–	71·9[b]

Data analysis was performed by ANCOVA. Different letters within a column show significant differences between rainfall groups at a 0·05 level. MI, moisture index; Total, in pooled data from FS and SFS; FS, fixed sandy land; SFS semi-fixed sandy land; Group 1, high-rainfall areas (sites 1–6, 14–16); Group 3, low-rainfall areas (sites 8–13, 17).

The data indicated that along a rainfall gradient ranging from 210 to 350 mm, sand and clay contents in fixed and semi-fixed sandy lands varied little with rainfall (sand content: $R^2 = 0{\cdot}001$, $P = 0{\cdot}89$; clay content: $R^2 = 0{\cdot}09$, $P = 0{\cdot}16$). Given a soil water content, soil water potential calculated from the soil water retention curves (Saxton *et al.*, 1986) based on soil texture also showed no significant variation along the rainfall gradient ($R^2 = 0{\cdot}04$, $P = 0{\cdot}38$). In contrast, leaf traits in this study varied significantly along the rainfall gradient (Figs S1 and S2). Furthermore, the results of ANOVA indicated that there were no significant differences in soil texture or soil water potential between low-rainfall areas (MI $\leq 0{\cdot}29$) and high-rainfall areas (MI $> 0{\cdot}29$) ($P = 0{\cdot}12$–$0{\cdot}59$), while relationships of SLA–N_{mass} and N_{area}–CC_{area} shifted significantly between the two rainfall areas (Figs 2 and 5). Therefore, the variations in leaf traits were mainly driven by rainfall but not by soil texture.

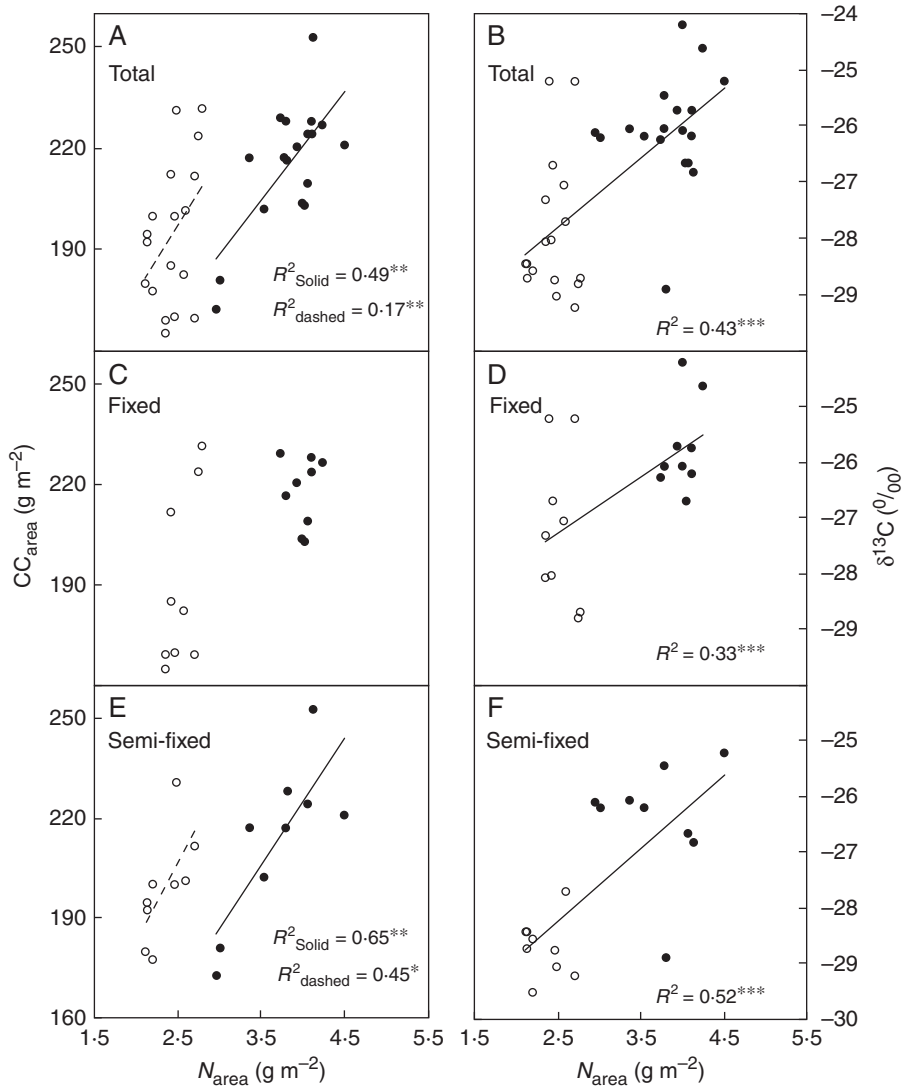

FIG. 6. The relationships of N_{area}–CC_{area} (A, C, E) and N_{area}–$\delta^{13}C$ (B, D, F) for *A. ordosica* along a rainfall gradient in the Qaidam Basin sandy lands. Empty circles and dashed trend lines are for the high-rainfall area (Qinghai Lake; rainfall, 401 mm; MI, 0·68); filled circles and solid trend lines are for the low-rainfall area (Dulan; rainfall 207 mm; MI, 0·25).

A new method to link leaf functional traits with arid vegetation zonation

According to the Vegetation Divisions of China (Editorial Committee for Vegetation of China, 1980; Zhang, 2007), the ecotone boundary between typical temperate and desert steppe zones is mainly determined by regional differences in annual rainfall, genus and species indicators, soil types, and dryland cropping systems, based on the realistic distribution map of natural and artificial vegetation. It is difficult to use such complicated indicators to predict the boundary change and to further understand the related mechanisms underlying the boundary formation. It has been demonstrated that leaf traits are useful for predicting ecosystem functions and processes at large scales (Schulze *et al*., 1994; Luo *et al*., 2009). Along an environmental gradient, variations in leaf traits affect plant adaptations to abiotic factors and therefore play an important role in determining plant species distribution patterns (Maharjan *et al*., 2011). There is evidence that leaf lifespan is a simple predictor of evergreen forest zonation in China (Zhang *et al*., 2010), but few studies have examined the linkage between leaf traits and arid vegetation zonation.

In this study, the leaf-trait data of *A. ordosica* indicated that the optimal balance of WUE and CC exists below a common climatic drought threshold (MI $\leq$ 0·29). This drought threshold of MI = 0·29 (with a transition between 0·30 and 0·32) corresponds well to the zonal boundary between typical and desert steppes in northern China (Fig. 7). As it is easy to measure leaf traits with repeatable sampling along a geographical transect, our findings suggest an operational way to link leaf functional traits with arid vegetation zonation. This is especially important to be able to detect and predict the dynamic vegetation change in arid and semi-arid regions due to climate change.

TABLE 5. *Differences in slopes and intercepts of* N_{area}-$\delta^{13}C$ *relationships for* A. ordosica *between rainfall groups in northern China sandy lands*

Group	MI	Slope			Intercept		
		Total	FS	SFS	Total	FS	SFS
Group 1	0·33–0·41	1·0[a]	0·71[a]	1·2[a]	−30·0[a]	−29·0[a]	−30·4[a]
Group 3	0·17–0·29	0·57[a]	0·51[a]	0·70[a]	−28·8[a]	−28·5[a]	−29·4[a]

Data analysis was performed by ANCOVA. Different letters within a column show significant differences between rainfall groups at a 0·05 level. MI, moisture index; Total, in pooled data from FS and SFS; FS, fixed sandy land; SFS semi-fixed sandy land; Group 1, high-rainfall areas (sites 1–6, 14–16); Group 3, low-rainfall areas (sites 8–13, 17).

SUPPLEMENTARY DATA

Supplementary data are available online at www.aob.oxfordjournals.org and consist of the following. Figure S1: Variations in SLA, N_{mass}, N_{area}, $\delta^{13}C$, CC_{mass} and CC_{area} for *A. ordosica* in fixed sandy land habitats along an MI gradient in northern China. Figure S2: Variations in SLA, N_{mass}, N_{area}, $\delta^{13}C$, CC_{mass} and CC_{area} for *A. ordosica* in semi-fixed sandy land habitats along an MI gradient in northern China.

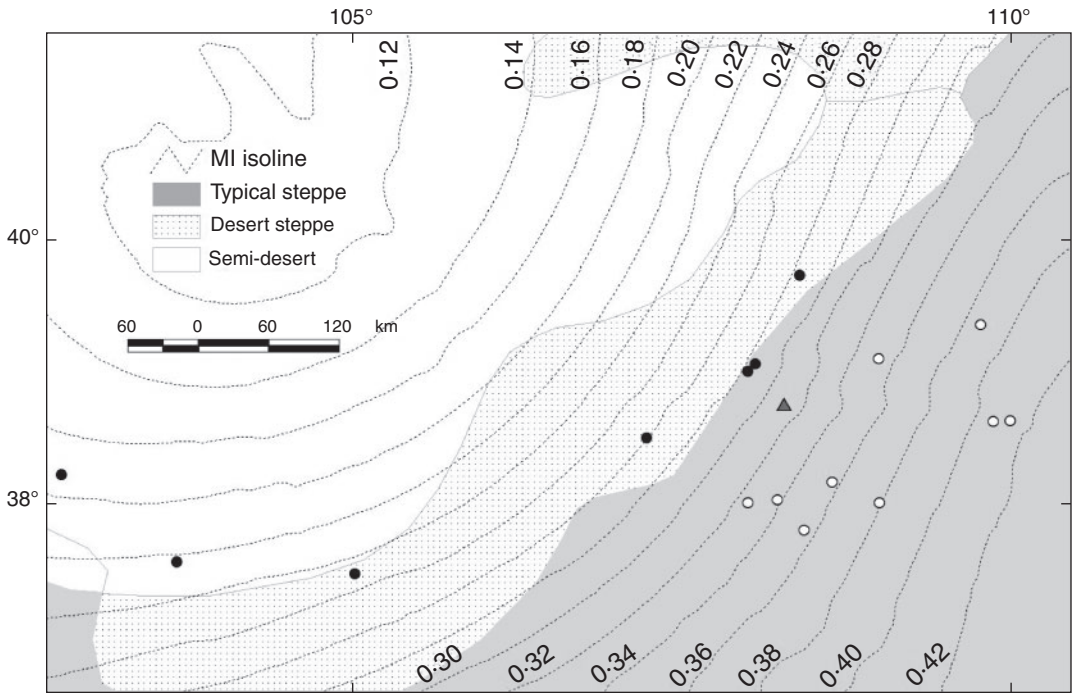

FIG. 7. The drought threshold (MI = 0·29) identified by leaf-trait data of *A. ordosica* corresponded well to the zonal boundary between typical temperate and desert steppes in Zhang (2007). Empty circles are the sites for high-rainfall areas (rainfall group 1, 310–370 mm; MI, 0·33–0·41); the grey triangle is the site for mid-rainfall transition (rainfall group 2, 290 mm; MI, 0·31); and filled circles are the sites for low-rainfall areas (rainfall group 3, 150–265 mm; MI, 0·17–0·29).

ACKNOWLEDGEMENTS

We thank J. H. Zhang, J. He and Q. L. Ma for their help in field data collection, and especially appreciate Dr I. J. Wright's insightful comments and suggestions for improving the manuscript. This study was funded by the National Natural Science Foundation of China (41301047), the Strategic Priority Research Program (B) of the Chinese Academy of Sciences (XDB03030402) and the State Ministry of Sciences and Technologies of China (2012BAD16B01).

LITERATURE CITED

Allen RG, Pereira LS, Raes D, Smith M. 1998. Crop evapotranspiration: guidelines for computing crop for water requirements. *FAO Irrigation and Drainage Paper 56*. Rome: FAO – Food and Agriculture Organization of the United Nations.

Amthor JS. 1989. *Respiration and crop productivity*. New York: Springer.

Baruch Z, Goldstein G. 1999. Leaf construction cost, nutrient concentration, and net CO_2 assimilation of native and invasive species in Hawaii. *Oecologia* **121**: 183–192.

Chapin FS III. 1989. The cost of tundra plant structures: evaluation of concepts and currencies. *American Naturalist* **133**: 1–19.

Chen FY, Luo TX, Zhang L, Deng KM, Tian XY. 2006. Comparison of leaf construction cost in dominant tree species of the evergreen broadleaved forest in Jiulian Mountain, Jiangxi Province. *Acta Ecologica Sinica* **26**: 2485–2493.

Chen LH, Li FX, Di XM, Zhao JX. 1998. *Aeolian sandy soils in China*. Beijing: Science Press.

Cornwell WK, Bhaskar R, Sack L, Cordell S, Lunch CK. 2007. Adjustment of structure and function of Hawaiian *Metrosideros polymorpha* at high vs. low precipitation. *Functional Ecology* **21**: 1063–1071.

Cui WC. 1991. *Artemisia ordosica* Krasch community in the semi-arid zone. *Grassland of China* **2**: 50–52.

Cunningham SA, Summerhayes B, Westoby M. 1999. Evolutionary divergences in leaf structure and chemistry, comparing rainfall and soil nutrient gradients. *Ecology* **69**: 569–588.

Duan ZH, Liu XM. 1995. Studies on aeolian sandy soil and its amelioration in Shapotou area at southern edge of Tengger Desert. *Arid Zone Research* **12**: 60–66.

Editorial Committee for Vegetation of China. 1980. *Vegetation of China*. Beijing: Science Press.

Farquhar GD, Ehleringer JR, Hubick KT. 1989. Carbon isotope discrimination and photosynthesis. *Annual Review of Plant Physiology and Plant Molecular Biology* **40**: 503–537.

Farquhar GD, Buckley TN, Miller JM. 2002. Optimal stomatal control in relation to leaf area and nitrogen content. *Silva Fennica* **36**: 625–637.

Field C. 1983. Allocating leaf nitrogen for the maximization of carbon gain: leaf age as a control on the allocation program. *Oecologia* **56**: 341–347.

Gower ST, Grier CC, Vogt KA. 1989. Aboveground production and N and P use by *Larix occidentalis* and *Pinus contorta* in the Washington Cascades, USA. *Tree Physiology* **5**: 1–11.

Griffin KL. 1994. Calorimetric estimates of construction cost and their use in ecological studies. *Functional Ecology* **8**: 551–562.

Groeneveld HW, Bergkotte M, Lambers H. 1998. Leaf growth in the fast-growing *Holcus lanatus* and the slow-growing *Deschampsia flexuosa*: tissue maturation. *Journal of Experimental Botany* **49**: 1509–1517.

Kjeldahl J. 1883. A new method for the determination of nitrogen in organic matter. *Zeitschrift fur Analytische Chemie Fresenius* **22**: 366–382.

Li ZH. 2007. *The research on granularity characteristics of the surface soil and erodibility particle in the desertification land in Inner Mongolia.* Master Degree Thesis, Inner Mongolia Normal University, Huhhot.

Luo TX, Zhang L, Zhu HZ, Daly C, Li MC, Luo J. 2009. Correlations between net primary productivity and foliar carbon isotope ratio across a Tibetan ecosystem transect. *Ecography* **32**: 526–538.

Maharjan SK, Poorter L, Holmgren M, Bongers F, Wieringa JJ, Hawthorne WD. 2011. Plant functional traits and the distribution of West African rain forest trees along the rainfall gradient. *Biotropica* **43**: 552–561.

Martínez F, Lazo YO, Fernández-Galiano RM, Merino JA. 2002. Chemical composition and construction cost for roots of Mediterranean trees, shrub species and grassland communities. *Plant, Cell & Environment* **25**: 601–608.

Merino J. 1987. The costs of growing and maintaining leaves of mediterranean plants. In: Tenhunen JD, Catarino FM, Lange OL, Oechel WC, eds. *Plant response to stress*. Berlin: Springer Verlag, 553–564.

Nagel JM, Griffin KL. 2001. Construction cost and invasive potential: comparing *Lythrum Salicaria* (Lythraceae) with co-occurring native species along pond banks. *American Journal of Botany* **88**: 2252–2258.

Nagel JM, Griffin KL, Schuster WS, *et al.* 2002. Energy investment in leaves of red maple and co-occurring oaks within a forested watershed. *Tree Physiology* **22**: 859–867.

Nagel JM, Huxman TE, Griffin KL, Smith SD. 2004. CO_2 enrichment reduces the energetic cost of biomass construction in an invasive desert grass. *Ecology* **85**: 100–106.

Penning de Vries FWT, Brunsting AHM, Van Laar HH. 1974. Products, requirements and efficiency of biosynthesis: a quantitative approach. *Journal of Theoretical Biology* **45**: 339–377.

Poorter H, De Jong R. 1999. A comparison of specific leaf area, chemical composition and leaf construction costs of field plants from 15 habitats differing in productivity. *New Phytologist* **143**: 163–176.

Poorter H, Villar R. 1997. The fate of acquired carbon in plants: chemical composition and construction costs. In: Bazzaz FA, Grace J, eds. *Plant resource allocation*. San Diego: Academic Press, 39–72.

Poorter H, Niinemets Ü, Poorter L, Wright IJ, Villar R. 2009. Causes and consequences of variation in leaf mass per area (LMA): a meta-analysis. *New Phytologist* **182**: 565–588.

Prentice IC, Dong N, Gleason SM, Maire V, Wright IJ. 2014. Balancing the costs of carbon gain and water transport: testing a new theoretical framework for plant functional ecology. *Ecology Letters* **17**: 82–91.

Reich PB, Walters MB, Ellsworth DS. 1997. From tropics to tundra: convergence in plant functioning. *Proceedings of the National Academy of Sciences USA* **94**: 13730–13734.

Saxton KE, Rawls WJ, Romberger JS, Papendick RI. 1986. Estimating generalized soil-water characteristics from texture. *Soil Science Society of America Journal* **50**: 1031–1037.

Schulze ED, Kelliher FM, Körner C, Lloyd J, Leuning R. 1994. Relationships among maximum stomatal conductance, ecosystem surface conductance, carbon assimilation rate, and plant nitrogen nutrition: a global ecology scaling exercise. *Annual Review of Ecology and Systematics* **25**: 629–660.

Smith WK, Vogelmann TC, DeLucia EH, Bell DT, Shepherd KA. 1997. Leaf form and photosynthesis. *BioScience* **47**: 785–793.

Song LY, Guang YN, Chen BM, Peng SL. 2007. Energetic cost of leaf construction in the invasive weed *Mikania micrantha* H.B.K. and its co-occurring species: implications for invasiveness. *Botanical Studies* **48**: 331–338.

Taiz L, Zeiger E. 1991. *Plant physiology*. Redwood City, CA: The Benjamin/Cummings Publishing Co., Inc.

Villar R, Merino J. 2001. Comparison of leaf construction costs in woody species with differing leaf life-spans in contrasting ecosystems. *New Phytologist* **151**: 213–226.

Wang C, Wang XB, Liu DW, *et al.* 2014. Aridity threshold in controlling ecosystem nitrogen cycling in arid and semi-arid grasslands. *Nature Communications* **5**: 4799, doi:10.1038/ncomms5799.

Wang LQ, Chen SH, Hao LZ. 2002. The study of ecological biological characters and geological distribution law of *Artemisia ordosica* Krasch. *Journal of Arid Land Resources and Environment* **16**: 95–98.

Wang TJ, Yang C, Ma J, Qiao SJ, Li DX. 2004. RAPD analysis on genetic differentiation of *Artemisia ordosica* populations. *Acta Scientiarum Naturalium Universitatis Neimongol* **35**: 399–403.

Wang Y. 2006. *Basic features of soil and vegetation and desertification evaluation of Artemisia ordosica sandy land.* Master Degree Thesis, Chinese Academy of Forestry, Beijing.

Wei HX, Wu B, Yang WB, Luo TX. 2011. Low-rainfall induced shift in leaf trait relationship within species along a semi-arid sandy land transect in northern China. *Plant Biology* **13**: 85–92.

Williams K, Percival F, Merino J, Mooney HA. 1987. Estimation of tissue construction cost from heat of combustion and organic nitrogen content. *Plant, Cell & Environment* **10**: 725–734.

Witkowski ETF, Lamont BB. 1991. Leaf specific mass confounds leaf density and thickness. *Oecologia* **88**: 486–493.

Wright IJ, Reich PB, Westoby M. 2001. Strategy shifts in leaf physiology, structure and nutrient content between species of high- and low-rainfall and high- and low-nutrient habitats. *Functional Ecology* **15**: 423–434.

Wright IJ, Reich PB, Westoby M. 2003. Least-cost input mixtures of water and nitrogen for photosynthesis. *American Naturalist* **161**: 98–111.

Wright IJ, Reich PB, Westoby M, *et al.* 2004. The world wide leaf economics spectrum. *Nature* **428**: 821–827.

Wright IJ, Reich PB, Cornelissen JHC, *et al.* 2005. Modulation of leaf economic traits and trait relationships by climate. *Global Ecology and Biogeography* **14**: 411–421.

Wu B, Ci LJ. 2002. Landscape change and desertification development in the Mu Us Sandy land, northern China. *Journal of Arid Environments* **50**: 429–444.

Zhang L, Luo TX, Daly C, Deng KM. 2010. Leaf life span as a simple predictor of evergreen forest zonation in China. *Journal of Biogeography* **37**: 27–36.

Zhang L, Luo TX, Liu XS, Wang Y. 2012. Altitudinal variation in leaf construction cost and energy content of *Bergenia purpurascens*. *Acta Oecologica* **43**: 72–79.

Zhang XS. 2007. *Vegetation of China and its Geographic Pattern: Illustration of the Vegetation Map of the People's Republic of China (1:1 000 000).* Beijing: Geological Publishing House.